Journal of Physics: Conference Series **555** (2014) 012018 doi:10.1088/1742-6596/555/1/012018

Extended Onshore Control of a Floating Wind Turbine with Wave Disturbance Reduction

S. Christiansen, T. Knudsen and T. Bak

Automation and Control, Department of Electronic Systems, Aalborg University, Fredrik Bajers vej 7C, 9220 Aalborg Øst, Denmark

E-mail: `sc@es.aau.dk`

Abstract. Reaching for higher wind resources beyond the water depth limitations of monopile wind turbines, there has arisen the alternative of using floating wind turbines. But the response of wave induced loads significantly increases for floating wind turbines. Applying conventional onshore control strategies to floating wind turbines has been shown to impose negative damped oscillations in fore–aft due to the low natural frequency of the floating structure. Thus, we suggest a control loop extension of the onshore controller which stabilizes the system and reduces the wave disturbance. The results shows that when adding the suggested control loop with disturbance reduction to the system, improved performance is observed in power fluctuations, blade pitch activity, and platform oscillations.

1. Introduction

As the interest in renewable energy increases, the means of harvesting and capturing wind energy have been continuously developed and improved. More reliable wind turbines make installation possible in harsher environments, such as offshore in shallow waters, where winds are stronger and hazards to human eyes and ears are less.

Floating wind turbines (FWT) are one of the latest developments in wind energy. The concept of a floating wind turbine extends the range of wind turbines beyond the limitations of monopile water depths, accessing deep water sites with potentially higher wind speeds and may offer wind energy to consumers in new regions.

A wind turbine installation has one simple objective: to produce cheap energy. However, if a wind turbine is operated to maximize power production regardless of fatigue loads, the lifetime of key components will significantly decrease and the cost of the energy will go up. This is especially important for a floating wind turbine, which by nature is influenced by a constant contribution of oscillations from wind and ocean waves. Therefore, a trade-off between maximum power production and minimum structural oscillation is required to minimize the total cost of the energy.

Applying conventional onshore control strategies to floating wind turbines has been shown to impose negative damped oscillations on the platform motion. The control must hence be adapted to the dynamic response of the floating structure. This can in principle be done by redesigning the entire control system or by adding control loops that extend the existing control system to handle the dynamics of a floating installation.

A number of results are available that redesign the control system. In [1], a tower damping control strategy was introduced using a wind estimator showing reduced tower oscillation at the cost of reduced power output. In [2] a detuned gain scheduled proportional integrating controller was applied. Linear quadratic control was applied in [3]. In [4, 5] wind and wave estimators were combined in a full range controller. In [6] a disturbance accommodating control was applied to reduce the wind disturbance.

All these results mentioned above rely on a redesigned control system. This paper takes a different approach, by suggesting a control loop extension to the onshore control without modifying the onshore controller. This provides potential benefits to manufacturers, as it simplifies the changes required in the control system to handle the floating installation. The

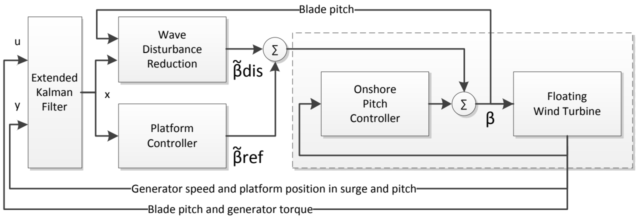

Figure 1. Overview of pitch control strategy. A Kalman filter is used to estimate the states and disturbance. The output of the onshore controller is corrected by improved feedback and wave disturbance reduction.

strategy is presented in Fig. 1. Note that the onshore pitch controller is left untouched, and the control redesign is merely an additional loop which acts on the onshore controller's output and stabilizes the system. Furthermore, disturbances from 1st and 2nd order wave induced moments are reduced by means of contrary blade pitch induced moments.

In Section 2.1, the closed loop stability of the onshore controller is investigated. In Section 2.2, a controller is designed to stabilize the system. In Section 2.3, a strategy is presented for reducing the wave disturbance in platform fore–aft. However, measuring wave disturbance is difficult. Thus, in Section 2.4, an estimate is made by designing an observer which models the wave induced moments as a stochastic process using an extended Kalman filter (EKF) [7]. In Sections 4 and 5, the results are presented and discussed. In Section 6, the contributions are concluded.

2. Methods

2.1. Closed Loop Stability of the Onshore Controller

The dynamics of a floating wind turbine is analyzed to determine the stability in platform pitch when applying onshore control. Only the wind is assumed to have a substantial impact on the dynamics. A model of platform translation and rotation in fore–aft is constituted by

$$\dot{\mathbf{x}}_\mathbf{s} = \mathbf{A}_\mathbf{s}\mathbf{x}_\mathbf{s} + \mathbf{B}_\mathbf{s}F_t, \tag{1}$$

where $\mathbf{x}_\mathbf{s} = [x_p \; \dot{x}_p \; \theta_p \; \dot{\theta}_p]^T$ represents the platform translational velocity $\dot{x}_p$ and rotational velocity $\dot{\theta}_p$. The aerodynamic thrust is defined by $F_t = \frac{1}{2}\sigma A v^2 C_t(\lambda, \beta)$, where σ is the density of air, v is the wind speed, C_t is the thrust coefficient, λ is the tip speed ratio, and β is the blade pitch angle. The tip speed ratio is defined by $\lambda = \Omega R/v$, where Ω is the rotor speed and R is the rotor radius.

The drivetrain is modeled by the first order system

$$I\dot{\omega} = -M_g + \frac{1}{N}M_a, \tag{2}$$

where ω is the generator speed, N is the gear ratio, M_g is the generator torque, and the aerodynamic torque is defined by $M_a = \frac{1}{2\Omega}\sigma A v^3 C_p(\lambda, \beta)$, where C_p is the power coefficient.

The available onshore controller is designed for systems with neglectable actuator dynamics, assuming that the dynamics of the actuators are insignificant in the closed loop system.

The onshore controller consist of a blade pitch controller and a generator controller. The pitch controller is a gain scheduled PI controller modeled by

$$\beta = \frac{1}{1+\frac{\beta}{\beta_k}} PI(\omega_{\text{ref}} - \omega), \tag{3}$$

where β is, as before, the blade pitch angle, β_k is a constant, and ω_{ref} is the generator speed reference. The onshore torque controller is modeled by

$$M_g = P_{\text{ref}}/\omega, \tag{4}$$

where P_{ref} is the power reference. The properties of these two controllers are specified in [8, 9].

Disregarding disturbances from the wind and waves, the combined dynamics of the platform, drivetrain, and controller is given by

$$\dot{\mathbf{x}} = f(\mathbf{x}, v), \tag{5}$$

where $\mathbf{x} = [\mathbf{x_s}^T\ \omega\ x_i]^T$, and x_i is an internal control state for integral control of the generator speed.

To determine its stability, the system is linearized by

$$\dot{\tilde{\mathbf{x}}} = \mathbf{A}\tilde{\mathbf{x}} = \frac{\partial f(\mathbf{x}, v)}{\partial \mathbf{x}} \tilde{\mathbf{x}}, \tag{6}$$

where $\tilde{\mathbf{x}} = \mathbf{x} - \bar{\mathbf{x}}$ describes the dynamics about an operating point $\bar{\mathbf{x}}$. The poles of the system are shown in Fig. 2, which show three conjugate pole pairs. The fastest closed loop poles are mostly related to the drivetrain, while the slowest are mostly related to translation of the platform and the unstable pair are mostly related to platform rotation.

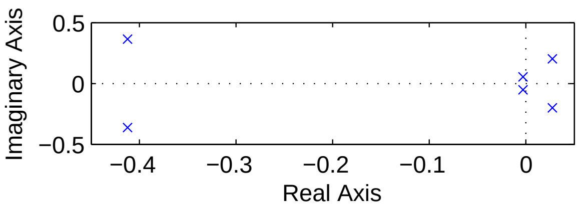

Figure 2. Closed loop poles of the FWT controlled by the onshore controller at 13 m/s.

2.2. Platform Controller

A platform controller is designed to stabilize the system by moving the unstable poles of the platform rotation in Fig. 2 to the left half plane. A new control signal β_{ref} is added to the output of the onshore controller as shown in Fig. 1, and the new system becomes

$$\dot{\tilde{\mathbf{x}}} = \mathbf{A}\tilde{\mathbf{x}} + \mathbf{B}\tilde{\beta}_{\text{ref}}. \tag{7}$$

The controller is based on state feedback by

$$u = -\mathbf{K}\tilde{\mathbf{x}}, \tag{8}$$

where $u = \tilde{\beta}_{\text{ref}}$. An LQ approach is used for stabilization and minimization of the perturbations of the system. The controller gain, $\mathbf{K}$, is found by minimizing the quadratic cost function

$$J = \int_0^\infty \left(\mathbf{x^T Q x} + u^T R u\right) dt, \tag{9}$$

where $\mathbf{Q}$ and R are weights to trade-off states and input perturbations.

The LQ controller is designed for the system in (7) for a wind speed of 13 m/s. Bryson's rule is used to determine the weights: $R = 1/90^2$ and $Q = [0\ 0\ 0\ 0\ 1/.03^2\ 1/\bar{\Omega}^2]$, which state that the blade pitch is allowed to vary by up to 90 degrees, while the platform rotational velocity is allowed to vary by up to 0.03 rad/s and the rotor speed is allowed to vary by up to $\bar{\Omega} = 12.1$ RPM.

In Fig. 3, the damping of the platform pitch is presented with and without the platform controller. The sudden dip in damping at 11.4 m/s is caused by the activation of the blade pitch controller. The platform controller is activated in the same region as the onshore controller, that is, above the rated wind speeds ($v > 11.4$ m/s). The response of the linearized onshore controller shows that the platform rotation stabilizes beyond 14 m/s. However, simulations using the nonlinear controller show that stability occur beyond 20 m/s. The mismatch is most likely caused by insufficient linearization of the gain-scheduled onshore controller.

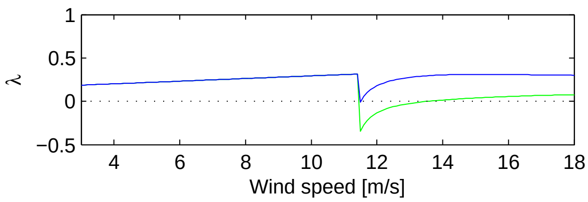

Figure 3. Comparison of damping ratio on platform rotation where green is the onshore controller and blue is the onshore controller with the platform controller.

The tuning of the platform controller is a matter of moving the green curve in Fig. 3 upward until the damping at all wind speeds is positive.

2.3. Wave Disturbance Reduction

The dynamical model of the combined system in (7–8) is extended to include the disturbance of hydrodynamic loads by

$$\dot{\tilde{\mathbf{x}}} = (\mathbf{A} - \mathbf{BK})\tilde{\mathbf{x}} + \mathbf{B_d}\tau_{\text{waves}}, \tag{10}$$

where τ_{waves} is the wave induced load on the platform. A blade pitch signal, β_{dis}, is designed to reduce the wave disturbance. This signal is added to the output of the onshore controller as shown in Fig. 1, and the system can be presented as

$$\dot{\tilde{\mathbf{x}}} = (\mathbf{A} - \mathbf{BK})\tilde{\mathbf{x}} + \mathbf{B_d}\tau_{\text{waves}} + \mathbf{B_p}\tilde{\beta}_{\text{dis}}, \tag{11}$$

where $\mathbf{B_p}$ translates the blade pitch to platform torque using the partial derivative of the aerodynamic thrust with respect to the blade pitch. The blade pitch signal, β_{dis}, is designed to reduce the wave disturbance by a factor of α, thus

$$\tilde{\beta}_{\text{dis}} = -\alpha \mathbf{B_p^{-1}} \mathbf{B_d} \hat{\tau}_{\text{waves}}, \tag{12}$$

where $\hat{\tau}_{\text{waves}}$ is the estimated wave disturbance.

2.4. State Estimation Using Extended Kalman Filter

The combined platform controller and wave disturbance reduction strategy requires full state feedback. However, wind speed and wave loads can be difficult to measure. Thus we suggest an EKF for estimating all states based on three outputs, which are

$$y = \begin{bmatrix} x_p & \theta_p & \omega \end{bmatrix}^T. \tag{13}$$

The wind speed and wave loads are modeled by stochastic processes.

The wave induced loads can be presented as $\tau_{\text{waves}} = \tau_{\text{waves1}} + \tau_{\text{waves2}}$ which are, respectively, the wave frequency dependent loads and the slowly varying drift loads. In [10], an empiric frequency dependent spectrum of the waves was presented as

$$S(\omega) = A\omega^{-5}e^{-B\omega^{-4}}, \tag{14}$$

where $A = 4\pi^3 H_s^2/(0.710T_0)^4$, $B = 16\pi^3/(0.710T_0)^4$, the average wave frequency is $\omega_0 = 2\pi/T_0$, the significant wave height is $H_s = 2.06v_d^2/g^2$, v_d is the developed sea wind speed, and g is the acceleration due to gravity. This spectrum is the modified Pierson–Moskowitz spectrum. Assuming the spectrum is constant, a linear stochastic model can be used to describe the combined wave induced loads by

$$\dot{\mathbf{x}}_{\mathbf{w}} = \mathbf{A}_{\mathbf{w}}\mathbf{x}_{\mathbf{w}} + \mathbf{B}_{\mathbf{w}}[w_1 \; w_2]^T \tag{15}$$

$$\tau_{\text{waves}} = \tau_{\text{waves1}} + \tau_{\text{waves2}} = \mathbf{C}_{\mathbf{w}}\mathbf{x}_{\mathbf{w}}, \tag{16}$$

where $w_{1,2}$ are Gaussian white noise processes and

$$\mathbf{A}_{\mathbf{w}} = \begin{bmatrix} 0 & 1 & 0 \\ -\omega_0^2 & -2\lambda_w\omega_0 & 0 \\ 0 & 0 & 0 \end{bmatrix} \tag{17}$$

$$\mathbf{B}_{\mathbf{w}} = \begin{bmatrix} 0 & 0 \\ K_w & 0 \\ 0 & 1 \end{bmatrix} \mathbf{C}_{\mathbf{w}} = \begin{bmatrix} 0 & X_i(\omega_0) & X_i(\omega_0) \end{bmatrix}, \tag{18}$$

where $X_i(\omega_0)$ is a wave frequency dependent constant which transforms the wave height to the wave induced load.

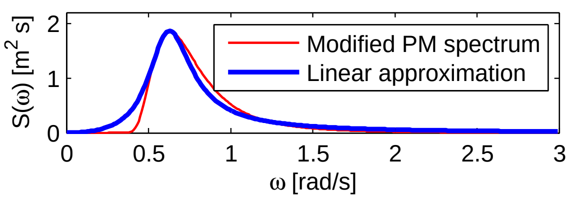

Figure 4. Modified Pierson–Moskowitz (PM) spectrum at $v = 13$ m/s and $\omega_0 = 0.8$ rad/s. The figure shows a comparison of the nonlinear and linearized spectrum related to the wave induced loads, τ_{waves1}.

To determine the unknown parameters K_w, λ_w, and ω_0, the modified Pierson–Moskowitz spectrum is linearized and in Fig. 4 a comparison is shown of the linearization and the original. Depending on the purpose, constant values for ω_0 and λ_w are suggested in [10]. From (14), it is acknowledged that the modified Pierson–Moskowitz spectrum depends on the developed sea wind speed and average wave frequency, which could be estimated by the EKF. However, variations of these are not considered in this paper.

The wind speed is $v = v_m + v_t$ where v_t is for turbulent wind and v_m is a slowly varying mean wind speed. These are modeled by

$$\dot{v}_t = \frac{-\pi v_m}{2L} v_t + w_3 \tag{19}$$

$$\dot{v}_m = w_4 \tag{20}$$

where t_i is the turbulence intensity and L is the turbulence length scale.

The EKF is designed to estimate the dynamics of the platform, drivetrain, waves, and wind, forming the state vector $\mathbf{x}_{\text{EKF}} = [\mathbf{x_s}^T\ \omega\ \mathbf{x_w}^{\mathbf{T}}\ v_t\ v_m]^T$. The EKF is implemented as described in [7]. The total system is defined by

$$\dot{\mathbf{x}}_{\text{EKF}} = f(\mathbf{x}_{\text{EKF}}, \mathbf{u}) + \mathbf{w} \tag{21}$$

$$y = [\ x_p \quad \theta_p \quad \omega\ ]^T, \tag{22}$$

where $\mathbf{u} = [M_g\ \beta]^T$.

The EKF consists of a time update part and a measurement update part, [11]. The time update uses information about the dynamics of the model and convariance to estimate the process.

$$\hat{x}_k^- = A\hat{x}_{k-1} + Bu_{k-1} \tag{23}$$

$$P_k^- = AP_{k-1}A^T + Q \tag{24}$$

Based on the time update, the measurement update corrects the estimated states taking into account the uncertainties in the states and the measurements.

$$K_k = P_k^- C^T (CP_k^- C^T + R)^{-1} \tag{25}$$

$$\hat{x}_k = \hat{x}_k^- + K_k(z_k - C\hat{x}_k^-) \tag{26}$$

$$P_k = (I - K_k C)P_k^- \tag{27}$$

3. Experimental Setup

3.1. Simulation Environment

The wind is simulated with a mean wind speed of 13 m/s, an air density of 1.225 kg/m^3, and a turbulence intensity of 10%.

The waves are simulated as irregular waves with a JONSWAP/Pierson–Moskowitz spectrum [12]. The significant wave height of the incident waves is 3.6 meters with a wave frequency of 10 seconds. The environmental conditions are simulated at a water depth of 320 meters and a water density of 1025 kg/m^3.

The waves are aligned with the direction of the wind. In Fig. 5, the wind speed and wave elevation used in the simulations are presented.

To reveal the system damping, the simulations were initialized at time zero in such a way that the floating wind turbine is released from an upright position and shortly after is forced backward by the wind and waves.

3.2. Software

The wind turbine is a three bladed upwind 5MW reference wind turbine specified by the NREL in [9], and implemented in the wind turbine simulation tool FAST, which is well recognized in the OC3 code benchmark, [13]. The implementation of the wind turbine installation consist of

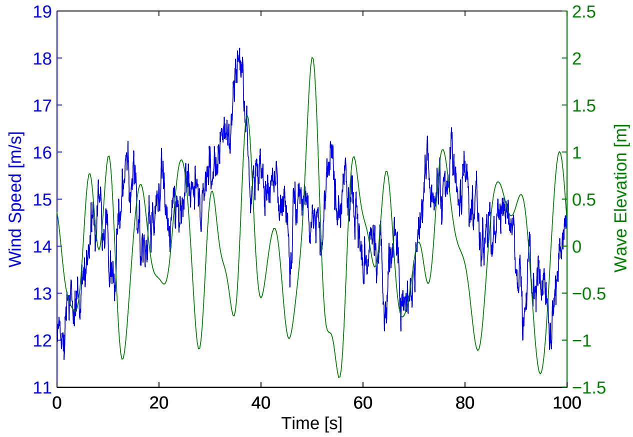

Figure 5. Wind speed and wave elevation used for the simulations. Wind and waves are aligned in the downwind direction.

a 5 MW wind turbine mounted on a ballast-stabilized buoy, to resemble an upscaled version of the 2.3 MW Hywind wind turbine. The floating wind turbine has a rotor radius of 63 meters, a tower height of 90 meters, and six degrees of freedom.

The simulations were performed in Simulink Matlab v7.9.0 (R2009b) linked with FAST v7.00.00a-bjj and AeroDyn v13.00.00a-bjj compiled for the OC3 Hywind running Windows 7 32bit.

4. Results

Based on the wind and wave environment in Fig. 5, the response of the onshore controller is presented with and without the platform controller. Furthermore, the result of adding wave disturbance reduction is presented. The disturbance is reduced by scaling factors of 0, 0.1, and 0.2, where a factor of 0 refers to the case of no disturbance reduction.

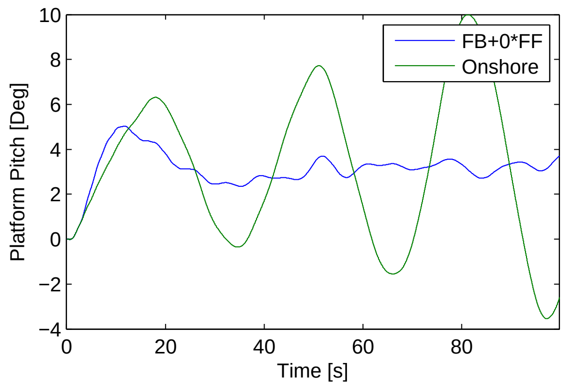

Figure 6. Comparing platform pitch responses using the onshore controller with platform controller (FB) without wave disturbance reduction (0*FF) and the onshore controller (Onshore). The mean wind speed is 13 m/s.

During these simulations the EKF estimate among others wind and wave induced moments on the platform which are presented in Fig. 7.

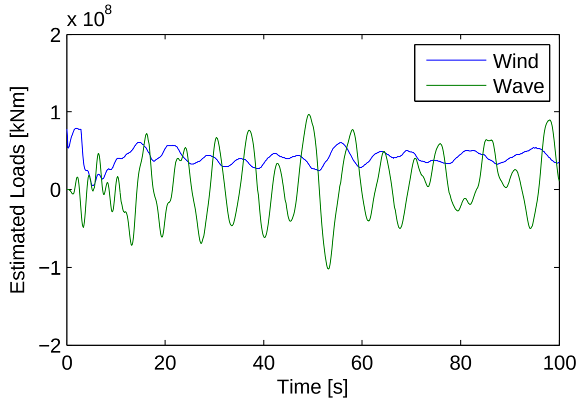

Figure 7. Torque induced by wind and waves, estimated during the simulation using the EKF.

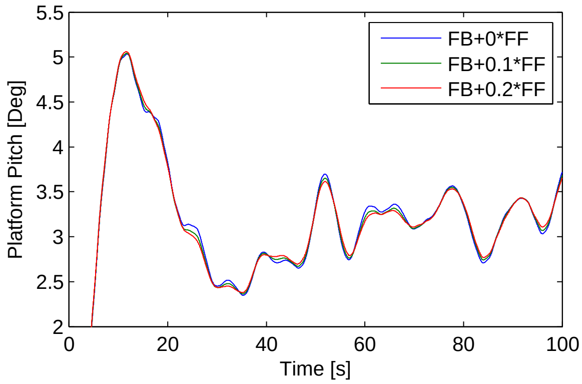

Figure 8. Comparing platform pitch response using onshore controller with platform controller (FB) including wave disturbance reduction (FF) scaled with factors of 0, 0.1, 0.2.

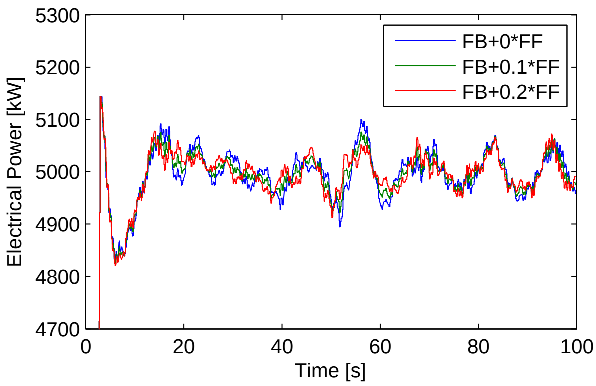

Figure 9. Comparing electrical power response using onshore controller with platform controller (FB) including wave disturbance reduction (FF) scaled with factors of 0, 0.1, 0.2.

5. Discussion

As expected from the analysis in Fig. 3, the response of the onshore controller shows an instability in the platform pitch in Fig. 6. However, when the platform controller is included, the system is stabilized. In Figs. 8–11, the disturbance reduction is added to the control system

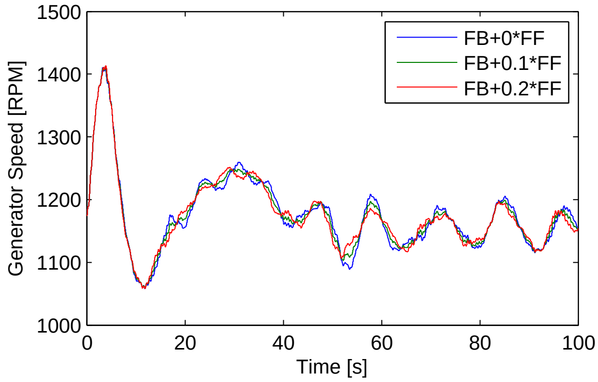

Figure 10. Comparing generator speed response using onshore controller with platform controller (FB) including wave disturbance reduction (FF) scaled with factors of 0, 0.1, 0.2.

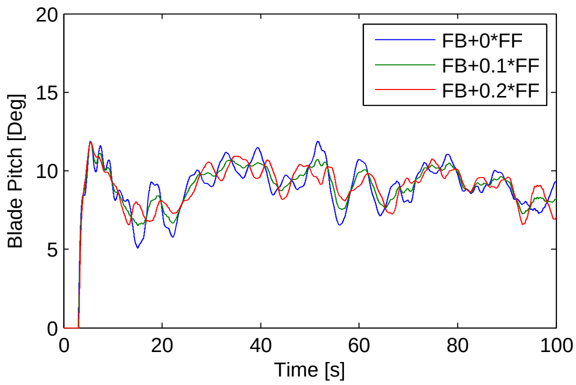

Figure 11. Comparing blade pitch response using onshore controller with platform controller (FB) including wave disturbance reduction (FF) scaled with factors of 0, 0.1, 0.2.

to reduce the wave disturbance. The results show that when adding disturbance reduction to the system, a reduction in power fluctuations, blade pitch activity, and platform oscillations is observed, improving the performance. Surprisingly, a reduction in actuation is achieved while improving performance in power and platform pitch. This can be explained by the fact that the disturbance reduction uses more information about the system. However, using a multi-objective control strategy is a trade-off between input and state perturbations.

Instead of manipulating the blade pitch output of the onshore controller, it might be more feasible to manipulate the existing speed reference to the onshore controller. This would leave a cleaner interface between the onshore controller and the platform controller.

6. Conclusion

The stability problem arising when onshore control is applied to a floating wind turbines has been addressed. The system has been analyzed and a platform controller has been suggested which stabilizes the system.

To accommodate wave disturbances, the wave induced moments on the platform were estimated, and the disturbance was reduced by using contrary blade pitch actuation. An extended Kalman filer was implemented to estimate the states, as is necessary for both the platform controller and the wave disturbance reduction. To achieve these estimates, Stochastic models for both the wind speed and the waves was implemented as a part of the filter.

Without redesigning the whole control system, the onshore controller has been preserved and an additional control loop was successfully designed to stabilize the system and reduce wave disturbance on a floating wind turbine.

7. Acknowledgment
This work was supported by the Norwegian Centre for Offshore Wind energy (NORCOWE).

References
[1] Skaare B, Hanson T D and Nielsen F G 2007 *Proceedings of 26th International Conference on Offshore Mechanics and Arctic Engineering*
[2] Jonkman J M 2008 *2008 ASME Wind Energy Symposium*
[3] Christiansen S, Knudsen T and Bak T 2011 *IEEE Multi-Conference on Systems and Control*
[4] Christiansen S, Bak T and Knudsen T 2012 *IEEE Transactions on Control Systems Technology - submitted*
[5] Christiansen S, Bak T and Knudsen T 2012 *IEEE Multi-Conference on Systems and Control*
[6] Namik H and Stol K 2009-483 *Proc. AIAA/ASME Wind Energy Symp.*
[7] Knudsen T, Soltani M and Bak T 2011 *Wind Energy* **14** 877–894 published online in Wiley Online Library (wileyonlinelibrary.com). DOI: 10.1002/we.491
[8] Jonkman J 2010 Definition of the floating system for phase iv of oc3 Tech. rep. NREL
[9] Jonkman J, Butterfield S, Musial W and Scott G 2007 Definition of a 5-mw reference wind turbine for offshore system development Tech. Rep. NREL/TP-500-38060 National Renewable Energy Laboratory
[10] Fossen T I 2011 *Handbook of Marine Craft Hydrodynamics and Motion Control* (WILEY)
[11] Welch G and Bishop G 2006 An introduction to the kalman filter Tech. rep. University of North Carolina at Chapel Hill
[12] Jonkman J M 2007 *Dynamics Modeling and Loads Analysis of an Offshore Floating Wind Turbine* Ph.D. thesis National Renewable Energy Laboratory
[13] Passon P, Khn M, Butterfield S, Jonkman J, Camp T and Larsen T J 2007 *The Science of Making Torque from Wind*